PAPER P

DIFFRACTED PROJECTIONS IN GEOTOMOGRAPHY

Jerry M. Harris

ABSTRACT

Recent advances in inverse scattering theory include the scattering effects of the first order Born or Rytov approximations. Diffraction tomography, as it is called, is generally formulated at a fixed monochromatic frequency and uses multiple views to sample the Fourier spectrum of the heterogeneous object profile. Image reconstruction is based on the generalized projection-slice theorem, which states that the Fourier transform of the scattered wavefield observed in a single plane wave experiment produces samples along a circular arc in Fourier space. The conventional projection-slice theorem is believed to breakdown when diffractive scattering was occurring.

We present a formulation of diffraction tomography which relates the amplitude of the scattered field to conventional straight line projections through the object profile, i.e., in a homogeneous background medium. These straight line projections are geometrically rotated relative to the conventional transmission ray projections which connect source and receiver points. Image reconstruction based on *diffracted projections*, as I call them, satisfy both the conventional projection-slice theorem and the generalized projection-slice theorem. Hence, conventional methods of image reconstruction can be used on problem involving diffraction. The diffracted projections are sampled using multifrequency observations of the scattered field at a fixed view.

INTRODUCTION

Conventional tomography uses a collection of ray optic (straight or curved ray) projections to reconstruct an inhomogeneous object profile. Reconstruction algorithms are based on the well-known projection-slice theorem or central-section theorem [1]. In high frequency applications, e.g., x-rays, the wavefield travels along straight ray paths connecting the source and receiver. The measured projections are simply line integrals through the profile of the object. The reconstruction algorithms either utilize the projections directly, e.g., convolution-backprojection techniques, or indirectly, e.g., transform methods.

In many new applications, however, such as medical ultrasound tomography and geophysical tomography, the probing wavefield cannot be modeled as simply propagating along rays connecting the source and detecor. Instead, the wavefield undergoes scattering, e.g., diffraction and refraction, the effects of which distorts the geometric projection. This distortion has been extensively studied and many researchers [2-8] use what is now called the generalized projection-slice theorem, which states that the Fourier transform of the scattered field measured along a straight line in object space yields samples along a circular arc in Fourier space. The perceived breakdown of the conventional projection-slice theorem has led to many new reconstruction algorithms loosely grouped and called diffraction tomography.

In this paper, we attempt to close the gap between conventional ray optic projection tomography and diffraction tomography by showing that the amplitude of the scattered field is related to a distorted set of straight line projections. These new projections, which we call diffracted projections, lie perpendicular to the bi-sectrix of the scattering vector rather than along the geometrical ray optic path connecting source and receiver. In the limit as the frequency increases toward infinity, or more specifically, as the wavelength goes to zero, the diffracted projection converges asymtoptically to the conventional ray optic projection. Although the concept of diffracted projections is not new, their explicit description and incorporation into a multi-static imaging algorithm as presented here is new. Concurrent with the work presented here, other researchers [6,7] have used a different approach to extract similar projections for wave equation based inversion methods.

Diffracted projections are sampled using multifrequency observations of the scattered field. Image reconstructions are performed using conventional techniques such as convolution-backprojection or transform methods. The most striking benefit of the diffracted projections is that one can apply the extensive developments of ray optic tomography to problems involving scattering.

THE FORWARD SCATTERING PROBLEM

We begin by formulating the forward scattering problem in two spatial dimensions for line sources. The derivation is similar to one given by Harris [9] for arrays of line sources or plane waves by Devaney [3]. The reduced wave equation for time-harmonic scalar waves is

$$(\nabla^2 + k^2)\, U(\mathbf{r},\mathbf{r}',\omega) = k^2\, O(\mathbf{r}) U(\mathbf{r},\mathbf{r}'\omega) \tag{1}$$

$U(\mathbf{r},\mathbf{r}',\omega)$ is the total time-harmonic scalar field of radian frequency w observed at the position $\mathbf{r} = (x,z)$ due to a line source at $\mathbf{r}' = (x',z')$. Without loss of generality, we consider arrays of sources and detectors located along the z-axis, at x' and x, respectively. This configuration, illustrated in Figure 1, is called crosswell. The function $O(\mathbf{r})$ on the right-hand-side of Eqn. (1) describes the inhomogeneous perturbations, i.e., object profile, in the medium. It is this object profile that we seek upon inversion. The object profile is related to the velocity of propagation in the medium through the equation

$$O(\mathbf{r}) = 1 - C_o^2 / C^2(\mathbf{r}). \tag{2}$$

where $C_o = \omega/k$ is the homogeneous background velocity of the medium. Although the object profile can depend on frequency, we will not consider such dependence here. In this paper, we will deal with multifrequency time-harmonic fields only.

The well-known first Born approximation for $U(\mathbf{r},\mathbf{r}',\omega)$ is

$$U(\mathbf{r},\mathbf{r}') = U_o(\mathbf{r}) + U_{sc}(\mathbf{r},\mathbf{r}') \tag{3}$$

$$U_{sc}(\mathbf{r},\mathbf{r}') = -k^2/4 \int d\mathbf{r}''\, O(\mathbf{r}'') U_o(\mathbf{r}'',\mathbf{r}') H_o(k|\mathbf{r}-\mathbf{r}''|) \tag{4}$$

where $H_o(kR)$ is the zero order Hankel function and $U_o(\mathbf{r},\mathbf{r}')$ is the field in the absence of any perturbations, i.e., the background field when $O(\mathbf{r})=0$.

Equally well-known is the fact that the fields in the Rytov approximation can be determined from the Born approximation [2,7]. For this reason, we will continue with results for the first-order Born approximation only, and point out when necessary, differences for the Rytov approximation.

For the single element line source, the background field incident upon the medium is given by the zero order Hankel function:

$$U_0(\mathbf{r},\mathbf{r}') = i\pi\, U_0(\omega)\, H_0(k|\mathbf{r}-\mathbf{r}'|) \tag{5}$$

where $U_0(\omega)$ is the complex Fourier amplitude of the incident wavefield. Harris [7] has shown that a plane wave decomposition of the Hankel functions, namely

$$H_0(k|\mathbf{r}-\mathbf{r}'|) = \pi^{-1} \int d\kappa \beta^{-1} \exp[+i\kappa(z-z') + i\beta(x-x')] \tag{6}$$

where $\beta^2 = k^2 - \kappa^2$ and x>x', followed by a 2D Fourier transform with respect to the source locations z' and the detector locations z, i.e.,

$$\tilde{U}_{sc}(x,\kappa;x',\kappa') = \iint dz dz'\, U_{sc}(x,z;x',z') \exp(-i\kappa' z' - i\kappa z) \tag{7}$$

reduces (4) for the scattered field to the following simplified expression:

$$\tilde{U}_{sc}(x,\kappa;x',\kappa') = \frac{\pi k^2}{\beta\beta'} \tilde{O}(\beta-\beta',\kappa+\kappa')\, U_0(\omega) \exp(-i\beta' x' + i\beta x) \tag{8}$$

In this equation, $\tilde{O}(\beta-\beta',\kappa+\kappa')$ is the 2D Fourier transform of the object profile O(x,z):

$$\tilde{O}(\kappa_x,\kappa_z) = \iint dx dz\, O(x,z) \exp(-i\kappa_x x - i\kappa_z z) \tag{9}$$

To perform the 2D Fourier transform indicated by (7), one must have a collection or array of sources and detectors. Eqn. (9), which provides a relationship between the 2D Fourier spectrum of the scattered field and the 2D spectrum of the object profile, is the basis of Fourier reconstruction techniques. This result is a statement of the generalized projection-slice theorem.

DIFFRACTED PROJECTIONS

We can reformulate the results of the previous section in terms of a new quantity I call diffracted projections. Diffracted projections are produced by a straight line integration through the object profile, though generally not along the transmission line connecting source and receiver. See (17) below. Our starting point is the two-dimensional Fourier spectrum of the scattered field, Eqn. (9). First, we must rewrite this equation into a more convenient form. To do this, we use a vector $\hat{\mathbf{s}}'$ to describe the angle of incidence and $\hat{\mathbf{s}}$ for the angle of observation in terms of the wavenumbers (β',κ') and (β,κ) :

$$k\hat{\mathbf{s}}' = \beta'\hat{\mathbf{x}} + \kappa'\hat{\mathbf{z}} \qquad k\hat{\mathbf{s}} = \beta\hat{\mathbf{x}} + \kappa\hat{\mathbf{z}} \qquad \mathbf{r}'' = x''\hat{\mathbf{x}} + z''\hat{\mathbf{z}} \tag{10}$$

With these definitions, the exponential factor in (9) becomes

$$(\beta - \beta')x'' + (\kappa + \kappa)z'' = \kappa_s \cdot \mathbf{r}'' \tag{11}$$

where

$$\kappa_s = k(\hat{\mathbf{s}} - \hat{\mathbf{s}}') \qquad \text{and} \qquad \kappa_s = 2k\sin(\theta/2) \tag{12}$$

The angle θ is defined by the equation $\cos(\theta) = \hat{s}\cdot\hat{s}' = (\beta\beta' + \kappa\kappa')/k^2$ is called the bistatic scattering angle. In forward scattering line-of-sight experiments, we have $\theta=0$. In backscattering experiments, we have $\theta=\pi$. See Figure 2. The two-dimensional Fourier transform of the object profile now becomes

$$\tilde{O}(\kappa_s) = \iint d\mathbf{r}''\, O(\mathbf{r}'') \exp[-ik(\hat{\mathbf{s}} - \hat{\mathbf{s}}')\cdot\mathbf{r}''] \tag{13}$$

The form of this equation is well known to those familiar far-field plane wave scattering theory.

The imaging procedure based on (9) or (13), widely reported in the literature, is to fix the radian frequency (ω) and vary the bistatic scattering angle θ in order to sample the spectrum of the object profile. This is commonly called single frequency multiview imaging. The inversion formula is found by inverting (8) for the spectrum of the object profile in terms of the scattered field, then inverting the Fourier transform, (9), for the profile itself. Results have been extensively reported [2,3,7].

Next, we place (13) in a more revealing form by making the following observation. Refer to Figure 2, where I illustrate the scattering diagram described by (13). For a given pair of incident and scattered wave directions, $\hat{\mathbf{s}}'$ and $\hat{\mathbf{s}}$, all scattering points $d\mathbf{r}''$ parallel to the scattering vector κ_s have the same phase. This suggests replacing the two-dimensional $\mathbf{r}''$ integration with integrations parallel and perpendicular to κ_s. The parallel path integration will have a phase factor of $2k\sin(\theta/2)$, whereas the perpendicular path integration will have a phase factor identically equal to zero. Thus the original integration is reduced to a series of slice integrals, each slice being a straight line projection perpendicular κ_s.

The construction outlined above amounts to changing coordinates from (x",z") to new coordinates (u,v) by rotating through the angle θ. In the new system, if I take the unit vector u parallel to the scattering vector, then v is perpendicular to κ_s:

$$\mathbf{u} = (\hat{\mathbf{s}} - \hat{\mathbf{s}}')k / \kappa_s = \hat{\mathbf{x}}(\beta - \beta')k / \kappa_s + \hat{\mathbf{z}}'(\kappa + \kappa')k / \kappa_s \qquad (15)$$

and $\mathbf{u} \cdot \mathbf{v} = 0$. This rotation reduces the factor given by (11) to $\kappa_s = \kappa_s \hat{\mathbf{u}}$ and (13) becomes

$$\tilde{O}(\kappa_s) = \tilde{P}(\kappa_s, \theta) = \int du\, P(\kappa_s, \theta) \exp(-i\kappa_s u) \qquad (16)$$

$$P(u, \theta) = \int dv\, O(u, v) \qquad (17)$$

The expression for the scattered field, (8), now becomes

$$\tilde{U}_{sc}(x, \hat{s}; x', \hat{s}') = \frac{\pi k^2}{\beta\beta'} \tilde{P}(\kappa_s, \theta)\, U_o(\omega) \exp(-i\beta' x' + i\beta x) \qquad (18)$$

Eqn. (18) gives the relationship between the 2D spectrum of the scattered field and the Fourier spectrum of the projections.

The quantity $P(u,\theta)$ is a straight line projection through the object profile O(x,z) at the angle $\theta/2$. We call $P(u,\theta)$ a "diffracted projection" because it is a geometric line integral in the usual sense yet it is the result of the wave effect of diffractive scattering. The diffracted projection does not lie along the geometrical transmission path connecting source and detector as in conventional ray tomography. Instead, for specified directions of incidence and observation, the diffracted projection lies parallel to the bisectrix of $\hat{s}'$ and $\hat{s}$ and perpendicular to the scattering vector κ_s as known in Figure 2.

In the Rytov approximation, the scattered field is expressed in terms of the complex phase Φ:

$$U_{sc}(\mathbf{r},\mathbf{r}') = U_o(\mathbf{r},\mathbf{r}')\exp[\Phi(\mathbf{r},\mathbf{r}')] \quad (19a)$$

The Fourier spectrum of the complex phase is related to the object profile through the equation

$$\tilde{\Phi}_{sc}(x,\hat{s};x',\hat{s}') = \frac{\pi k^2}{\beta\beta'}\tilde{P}(\kappa_s,\theta)\, U_o(\omega)\, \exp(-i\beta' x' + i\beta x) \quad (19b)$$

Devaney [3] has shown that in the limit as the wavelength goes to zero ($k \to \infty$) the phase factor Φ reduces to a line integral along the ray optics path. This is easy to see from (19). In the limit as $k \to \infty$, the spectrum $\tilde{\Phi}_{sc}$ becomes more and more compact, eventually becoming significantly different from zero only near $\hat{s}' \sim \hat{s}$, the forward scattering direction. Thus, the vector $\hat{v}$ asymtoptically approaches $\hat{s}$ and $\hat{u}$ perpendicular to $\hat{s}'$. The diffracted projection converges to the conventional ray optic projection connecting the source and detector.

SAMPLING DIFFRACTED PROJECTIONS

In single frequency multiview diffraction tomography, the spectrum is sampled by varying the bistatic scattering angle θ while holding the frequency fixed. This produces samples in Fourier space along circular arcs as shown in Figure 3a. This arc, rather than a straight line, results from the trigonometric relationships, (11) and (12), connecting the scattering vector and the angles of incidence and observation. This arc feature is the basis for the so-called generalized projection-slice theorems of diffraction tomography. As shown above however, the Fourier transform of the scattered field given in equations (8) or (19) is also given in terms of the diffracted projections. To sample the projections directly, one must vary κ_s in a manner that holds θ constant. This is accomplished by varying the frequency w for fixed scattering geometry as can be seen from the equation for κ_s.

Multifrequency observations of the scattered field yield samples in Fourier space which lie along a straight line through the origin as shown in Figure 3b. In this case, the magnitude of the scattering vector is proportional to the independent frequency variable w. Thus the conventional and well-known projection-slice theorem applies to the reconstruction problem. The widely advanced belief that diffraction phenomena can not be easily handled within the framework of conventional tomography is false. By using diffracted projections, one can apply, with little more than coordinate transformations, the vast developments in conventional ray tomography to problems involving diffraction. By using a combination of multiview and multifrequency observations, one obtains the Fourier transform of the object's projections with samples organized along a polar grid as shown in Figure 3b.

CONCLUSION

We have presented a formulation of diffraction tomography which relates the multifrequency amplitude of the scattered field to distorted straight line projections through the object profile. We call these new straight line projections diffracted projections because they include first order diffraction effects. Like conventional ray transmission projections which connect the source and receiver, the diffracted projections readily lend themselves to conventional methods of image reconstruction based on the conventional projection-slice theorem. In general, the diffracted projections lie parallel to the angle made by the bisectrix of the incidence and observation vectors rather than along the geometrical optics path connecting the source and detector. In the limit however, as the probing wavelength goes to zero, the diffracted projection converges asymtoptically to the ray optic transmission projection.

REFERENCES

[1] R. M. Lewitt, "Reconstruction Algorithms: Transform Methods," Proc. IEEE, vol 71, no. 3, pp. 390-408, March 1983.

[2] J.K. Greenleaf, "computerized Tomography with Ultrasound," Proc. IEEE, Vol 71 no. 3, March 1983

[3] A. J. Devaney, "Geophysical Diffraction Tomogrpahy," IEEE Trnas. Geoscien. Remote Sens., vol. Ge-22, no. 1, pp. 3-13, Jan 1984.

[4] S. K. Kenue and J. F. Greenleaf, "Limited Angle Multifrequency Diffraction Tomography," IEEE Trans. Sonic Utrason., vol. SU-29, no. 8, pp. 2132-217, July 1982.

[5] S. J. Norton and M. Linzer, "Ultrasonic Reflectivity Imaging in Three Dimensions," IEEE Trans. Biomed. Eng. BME-28, pp. 202-220, 1981.

[6] G. Emersoy, M. Oristaglio and B. Levey, J. Acoust. Soc. Am, 1985.

[7] J. M. Harris, "Diffraction Tomographic Imaging with Arrays of Line Sources and Detectors," IEEE Trnas. Geoscien. Remote Sens., vol. Ge-25, no. 4, pp. 448-455, July 1987.

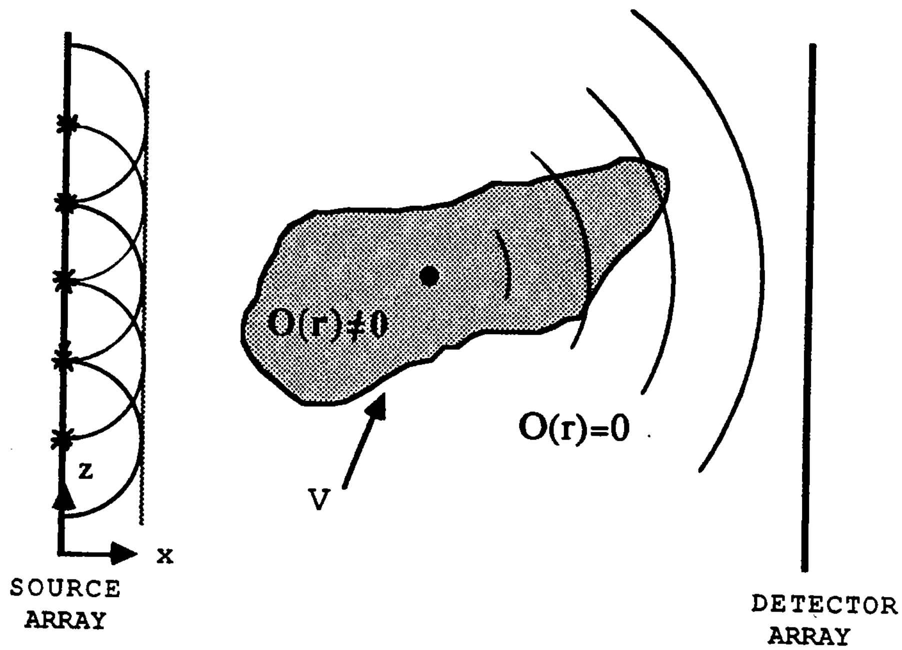

Figure 1. Model for scattering of an acoustic wave by heterogeneous region of compact support O(**r**). The incident field is generated by an array of line sources.

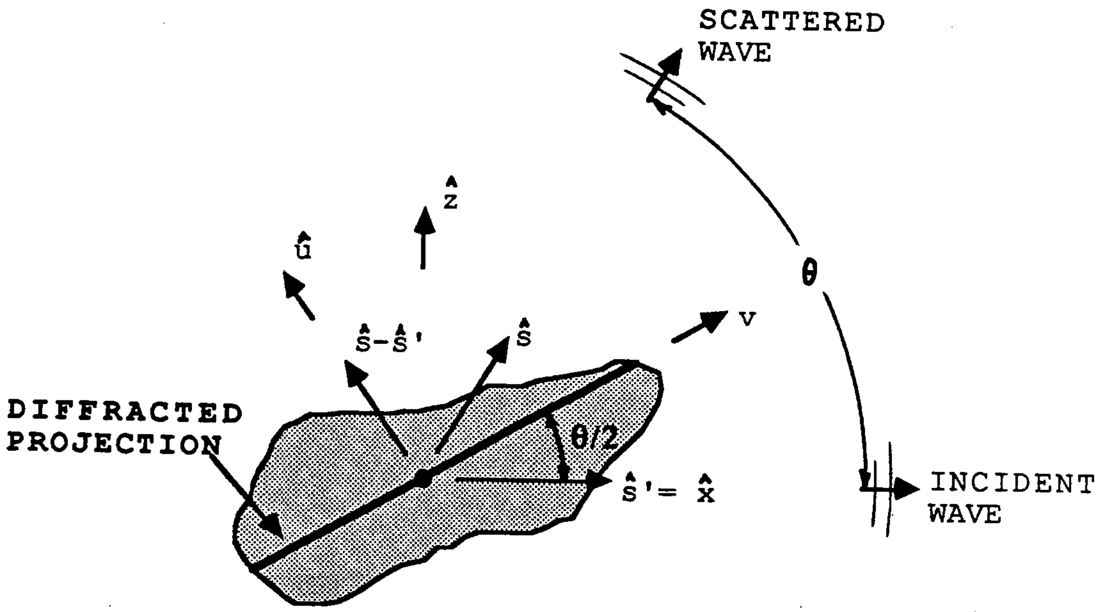

Figure 2. Diffracted projections are formed perpendicular to the bisectrix of the incident and observation vector. The limiting cases are backscattering where the diffracted projections are perpendicular to the reflected ray path and forward scattering where the diffracted projections are parallel to the transmitted paths.

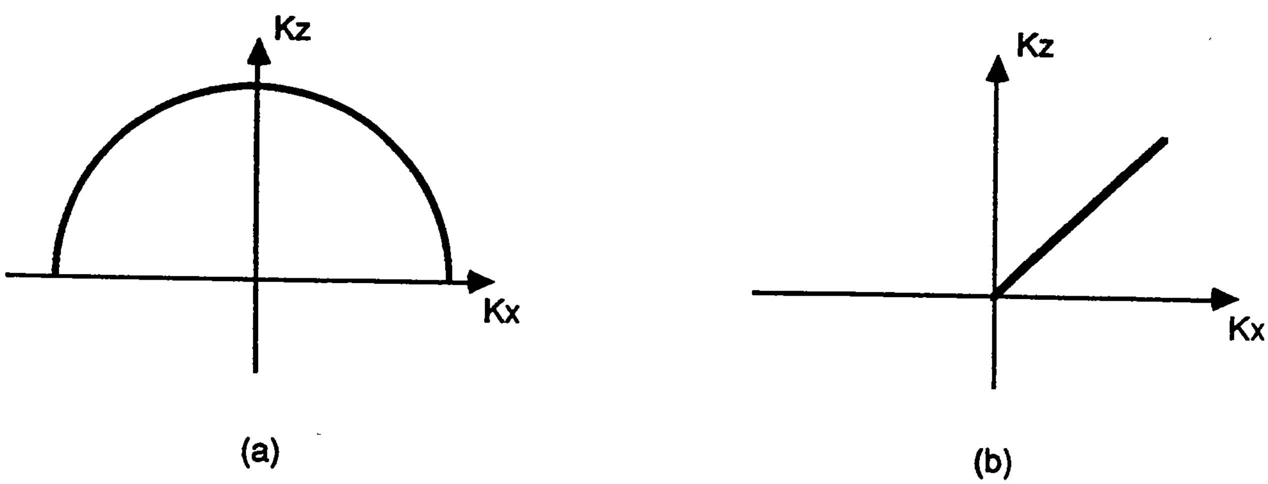

Figure 3. (a) Single frequency, multi-view diffraction tomography samples the object's Fourier space along circular arcs. (b) Diffracted projections are easily sampled by multifrequency observations that give straight line samples in Fourier space.